Perovskite- Hematite Tandem Cells for Efficient Overall Solar Driven Water Splitting

ARTICLE *in* NANO LETTERS · MARCH 2015

Impact Factor: 13.59 · DOI: 10.1021/acs.nanolett.5b00616

1 AUTHOR:

Guru Dayal
Nanyang Technological University
1 PUBLICATION **2** CITATIONS

SEE PROFILE

Communication

Perovskite- Hematite Tandem Cells for Efficient Overall Solar Driven Water Splitting

Gurudayal *, Dharani Sabba, Hemant Kumar Mulmudi, Lydia H. Wong, James Barber, Michael Grätzel, and Nripan Mathews

Nano Lett., **Just Accepted Manuscript** • DOI: 10.1021/acs.nanolett.5b00616 • Publication Date (Web): 30 Mar 2015

Perovskite- Hematite Tandem Cells for Efficient Overall Solar Driven Water Splitting

Gurudayal [1], Sabba Dharani [2], Mulmudi Hemant Kumar [2], Lydia Helena Wong [1], James Barber [1,3], Michael Grätzel [4], and Nripan Mathews [1,2]*

[1] School of Materials Science and Engineering, Nanyang Technological University, Nanyang Avenue, Singapore 639798.

[2] Energy Research Institute @NTU (ERI@N), Research Techno Plaza, X-Frontier Block, Level 5, 50 Nanyang Drive, Singapore 637553.

[3] Department of Life Sciences, Imperial College London, London, UK

[4] Laboratory of Photonics and Interfaces, Department of Chemistry and Chemical Engineering, Swiss Federal Institute of Technology, Station 6, CH-1015 Lausanne, Switzerland.

ABSTRACT:

Photoelectrochemical water splitting half reactions on semiconducting photoelectrodes have received much attention but efficient overall water splitting driven by a single photoelectrode has remained elusive due to stringent electronic and thermodynamic property requirements. Utilising a tandem configuration wherein the total photovoltage is generated by complementary optical absorption across different semiconducting electrodes is a possible pathway to unassisted overall light induced water splitting. Due to the low photovoltages generated by conventional photovoltaic materials (eg. Si, CIGS), such systems typically consist of triple junction design which increases the complexity due to optoelectrical trade-offs and are also not cost effective. Here we show that a single solution processed organic-inorganic halide perovskite ($CH_3NH_3PbI_3$) solar cell in tandem with a Fe_2O_3 photoanode can achieve overall unassisted water splitting with a solar to hydrogen conversion efficiency of 2.4%. Systematic electro optical studies were performed to investigate the performance of tandem device. It was found that the overall efficiency was limited by the hematite's photocurrent and onset potential. To understand these limitations, we have estimated the intrinsic solar to chemical conversion efficiency of the doped and undoped Fe_2O_3 photoanodes. The total photopotential generated by our tandem system (1.87V) exceeds both the thermodynamic and kinetic requirements (1.6V), resulting in overall water splitting without the assistance of an electrical bias.

KEYWORDS: Perovskite solar cells, Unassisted water splitting, $CH_3NH_3PbI_3$, Tandem, Hematite, Photoelectrochemical cell

INTRODUCTION

The growing need for affordable clean energy to combat excessive use of fossil fuels has motivated the scientific community to develop various ways of harnessing solar energy including photovoltaics (PV) and photoelectrochemical (PEC) fuel generation.[1] Solar fuels have been demonstrated to be advantageous in storing solar energy in the form of chemical bonds such as in H_2 through the PEC splitting of water to provide a net supply of reducing equivalents.[2 3] Based on the free energy change required to split one molecule of H_2O to H_2 and ½ O_2 under standard conditions (237.2 kJ/mol) as well as the kinetic barriers associated with oxygen and hydrogen evolution reactions, about 1.8 - 2.0V of solar generated photopotential is necessary.[4-7] In principle this potential requirement could be obtained from an semiconductor with appropriate valence and conduction bands illuminated by visible light. Such a reaction involves the use of a single semiconductor which absorbs two photons (S2) to generate a molecule of H_2. However, designing an S2 system which generates carriers of high photopotential, while possessing appropriate energy levels to drive the water splitting reaction has proven challenging. Increasing the bandgap of the semiconductor to generate a higher photopotential results in poorer solar absorption and reduced photocurrents. These energetic limitations along with the critical aqueous stability problem have not been efficiently met by a single semiconductor based system. A more flexible approach involves a dual bandgap absorber system which utilizes a total of 4 photons (D4) to (produce a molecule of H_2) realize solar water splitting. Such a tandem PEC system can consist of a photoanode/photocathode design or a photoelectrode/photovoltaic design. This tandem approach is similar to the Z-scheme of natural photosynthesis in which two

semiconductors with different absorption spectra can address a broad part of the solar spectrum and deliver a high solar to hydrogen (STH) efficiency for water splitting.[8-11] A notable effort in realising the D4 design employed a $GaInP_2$/GaAs configuration which displayed a high STH efficiency of 12.5%, but suffered from high costs and low stability.[12] Sivula and coworkers have also demonstrated a single dye sensitized solar cell in a tandem configuration with a STH efficiency of 1.17%.[11] Due to the low operational voltages of conventional photovoltaic systems (Si, CuInGaS/Se), many of the D4 designs have required the series integration of several solar cells to generate the photopotential required for splitting water.[13-15] These complicated approaches require a careful balance of the optical absorption and photocurrent generation within each solar cell to drive the overall reaction efficiently. Moreover, such architectures should also balance performance against fabrication complexity in order to allow for economical solar hydrogen production.

While designing a D4 system for efficient water splitting, the choice of the photoelectrode is critical. Hematite (Fe_2O_3) is an economically viable, aqueous stable semiconductor with a suitable bandgap for catalysing the oxygen evolution reaction using visible light.[16-19] The maximum solar-to-hydrogen conversion efficiency of hematite is predicted to be 16.8%.[20, 21] However the short hole diffusion lengths and sluggish kinetics of hole injection, limit the performance of hematite.[5, 22] More critically, the position of its conduction band is not favourable for H_2 reduction, requiring an external bias to drive the complete water splitting reaction.[23, 24] Choosing a solar cell that can drive the hematite photoelectrode for unassisted water splitting requires two criteria to be satisfied- a significant photovoltage and sufficient spectral mismatch. Since Fe_2O_3 has a bandgap of 2.1 eV, the semiconductor utilised in the solar cell should possess a smaller bandgap for absorption in the red end of the solar spectrum and still be able to provide

sufficient photovoltage. From an economic point of view, the solar cell should be easy to fabricate through simple solution based processes.

Here, we demonstrate that a *single* organic-inorganic halide perovskite ($CH_3NH_3PbI_3$) solar cell can fulfil these requirements and be utilised to drive photoelectrochemical water splitting. Solution processed $CH_3NH_3PbI_3$ has created a revolution in the area of photovoltaics, with efficiencies of up to 20% achieved in the last 2 years.[25, 26] Impressively, the open circuit voltages noted in these solar cells have been close to 1V (approaching **its** bandgap of 1.55eV), pointing to its excellent charge transport properties and low recombination rates.[27, 28] Therefore an ideal way of performing unassisted water splitting using hematite photoanode can be realized by stacking the photoelectrode with a perovskite solid state solar cell which has an extended optical absorption up to ~800 nm. The high open circuit voltage of perovskite solar cells can be exploited to drive water splitting by connecting both the hematite photoanode and perovskite solar cell in series. Recently, Gratzel and coworkers have demonstrated that two simultaneously illuminated perovskite solar cells can drive an earth abundant NiFe electrocatalyst for water splitting.[29] However, a true tandem photoelectrochemical cell would require that the photovoltage be generated by the water splitting photoelectrode as well as by the photovoltaic cell with each absorber addressing distinct parts of the solar spectrum.

In this report, we reveal a tandem device containing a single perovskite solar cell and doped hematite photoanode with a STH efficiency of 2.4%. To the best of our knowledge, this is the highest efficiency achieved in a system incorporating a single solar cell and a Fe_2O_3 water splitting photoelectrode. We have employed cost effective solution processable fabrication methods (spin coating, hydrothermal method) to fabricate perovskite solar cells and nanostructured Mn doped hematite photoanodes. Mn doped hematite photoanode provides a

higher photovoltage which in series with the photovoltage of the perovskite solar cell enables light driven water splitting in the absence of an external potential bias.

EXPERIMENTAL SECTION

(i) Hematite Photoanode:

Hematite nanorod array photoanodes were grown on a fluorine-doped tin oxide (FTO, Nippon Sheet Glass Co Ltd, 15 ohm/sq, 1×2.5 cm) substrate. The hematite nanorods were prepared by a procedure modified from our previous work.[30] To grow the nanowires, 10 ml of aqueous solution containing 1.5 mmol $FeCl_3$•$6H_2O$ (Sigma-Aldrich) and 1.5 mmol urea (Sigma-Aldrich) was transferred into a 20 mL Teflon lined autoclave and for Manganese doping 5 mol percent $MnCl_2$•$4H_2O$ precursor was added during the hydrothermal synthesis. The substrates were placed with the FTO side facing the wall of the autoclave at an angle of about 45 degrees. After 6 hrs of reaction at 100 °C, a uniform FeOOH film was formed on the FTO substrate. The substrates were thoroughly rinsed with DI water. A 0.1 M iron acetylacetonate precursor in ethanol was sprayed on to the FeOOH nanorods at 525 °C and finally annealed at 550 °C for 2 hrs to convert FeOOH to a hematite film in ambient air atmosphere. The samples were further annealed at 750 °C for 20 min in argon for photoelectrochemical (PEC) measurements. An oxygen evolution catalyst Co-Pi has been photoelectrodeposited on annealed hematite photoanodes (both pristine and Mn-doped) at 0.4 V vs. Ag/AgCl for 15 sec.

(ii) Perovskite solar cell:

For the fabrication of the perovskite solar cell, 2.2 mm thick, Pilkington FTO glass substrates, with a sheet resistance of <14 ohm/square were used. The desired pattern was laser etched and

cleaned by ultra-sonication in decon soap solution followed by subsequent rinsing with DI water and ethanol. The substrates were further ultrasonicated in ethanol for 15 min and then dried by using nitrogen gas. A thin (80-100 nm) and compact TiO_2 blocking layer was deposited on these cleaned and etched FTO by aerosol spray pyrolysis of a diluted solution of titanium diisopropoxide bis (acetylacetonate) (75 wt. % in isopropanol (IPA)) using ambient air as carrier gas. The titanium diisopropoxide bis (acetylacetonate) solution was diluted with absolute ethanol in the 1: 9 ratio by volume. These substrates were then immersed in 0.1 M titanium tetra chloride ($TiCl_4$) solution at 70 °C for 1 h followed by annealing at 500 °C for 1 h. Then 1.5 x 2 cm of these substrates were masked with tape on either sides partly covering the laser etched area and the FTO. On the exposed area, diluted TiO_2 paste (DSL 30 NRD, Dyesol, 1:3.5 by weight in absolute ethanol) was spin coated at 4000 rpm for 30s followed by annealing at 120 °C for 10 min and 500 °C for 15 min. The TiO_2 films were subjected to 20 mM $TiCl_4$ solution at 70 °C for 30 min followed by rinsing with DI water and ethanol. 1 M of lead iodide (PbI_2) solution in N,N-dimethyl formamide (DMF) was spin coated at 6000 rpm for 5 s inside the glove box followed by immersion in methyl ammonium iodide (CH_3NH_3I) solution (8 mg/mL in isopropanol (IPA)) for 20 min in dry box (relative humidity < 15 %) for the formation of perovskite layer on the mesoporous films. The perovskite loaded films were then spin coated at 4000 rpm and dried at 100 °C for 30 min. The widely used hole transporting material (HTM) namely spiro-OMeTAD (2, 2', 7, 7'-tetrakis-(N, N-di-p-methoxyphenylamine) 9, 9'-spirobifluorene) was used in chlorobenzene (100 mg/mL) with additives like Li $(CF_3SO_2)_2N$ (520 mg/mL in acetonitrile), tert-butylpyridine (48 µL) and FK102 dopant (10 mol% in acetonitrile (ACN)). The HTM was spin coated at 4500 rpm for 30 s inside the dry box and finally the gold (Au) contacts were deposited by thermal evaporation yielding an active area of 0.2 cm^2.

CHARACTERIZATION AND MEASUREMENTS

PEC measurements were performed using CHI 660D working station (CH Instruments, Inc.) in three-electrode and two electrode electrochemical configurations with 1 M NaOH (pH=13.6) electrolyte. Platinum coil and Ag/AgCl were employed as counter and reference electrodes, respectively. The working surface area of the photoelectrode was 0.12 cm^2. The light source was a 150 W Xenon lamp (67005, Newport Corp.) equipped with a solar filter (KG 3) with a measured intensity equivalent to standard AM 1.5G sunlight (100 $mWcm^{-2}$) on the sample surface. Incident photon to current conversion efficiency (IPCE) characteristics were measured with a Xenon light source (MAX-302, Asahi Spectra Co. Ltd.) coupled with a monochromator (CMS-100, Asahi Spectra Co. Ltd.) from 305 to 600 nm, at a potential of 1.23 V vs. RHE. A calibrated Si photodiode (Bentham, DH-Si) was used to calculate the IPCE of the hematite photoanodes. A source meter (Keithley Instruments Inc., Model: 2400) was used to measure the photocurrent of Si diode. The working station (CHI 660D, CH Instruments, Inc.) mentioned above was used to measure the photocurrent of samples.

RESULTS AND DISCUSSION

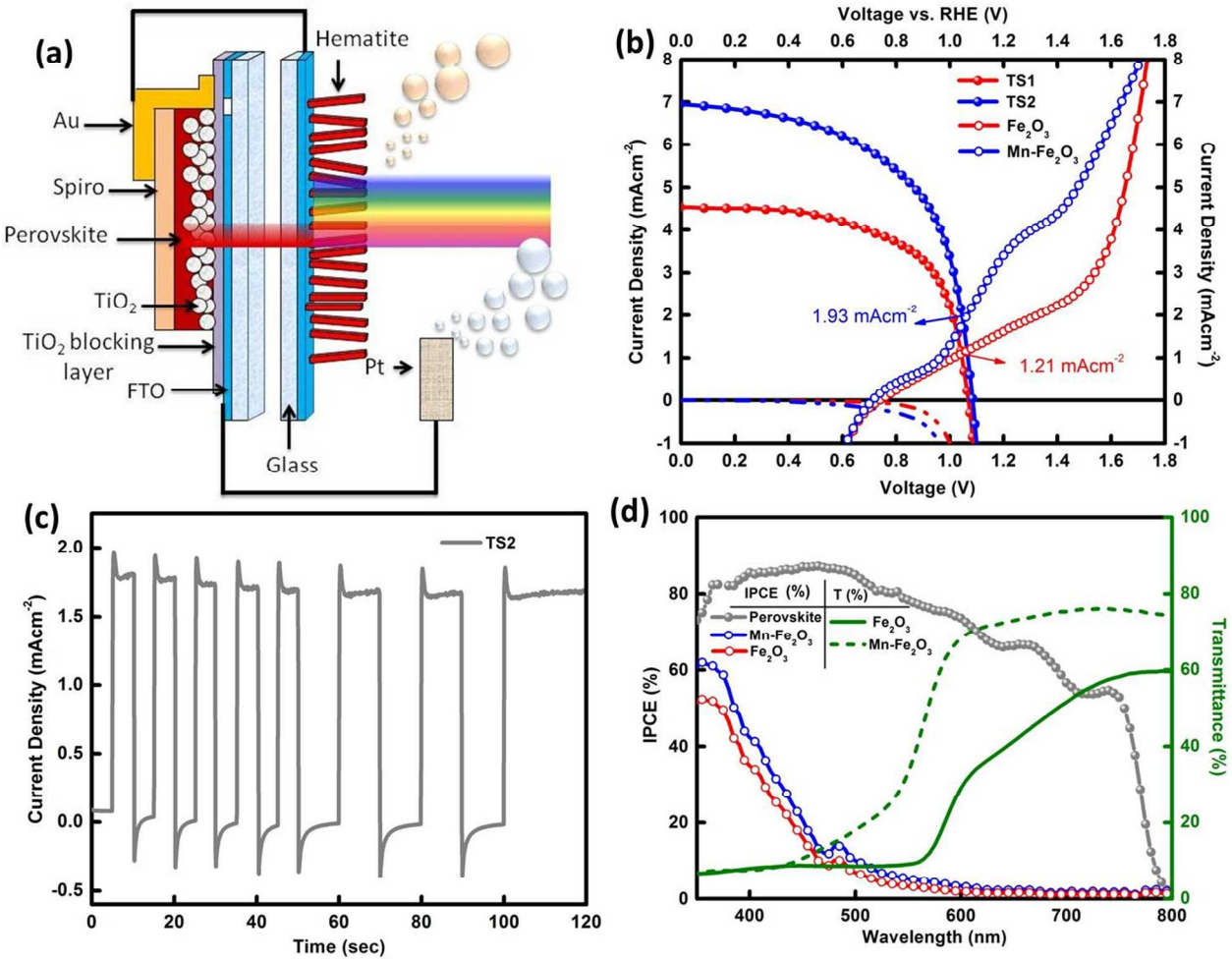

Figure 1. (a) Schematic of the dual junction perovskite solar cell/ hematite photoanode tandem cell, (b) Current-Voltage curve of a perovskite solar cell-hematite photoanode tandem devices together under standard AM 1.5G irradiation, (c) I-t curve of tandem cell (TS2) in 1 M NaOH electrolyte under 1 Sun AM1.5G (100mWcm^{-2}) up to 120 sec (d) IPCE spectra of hematite

photoanodes (pristine and Mn doped) and perovskite solar cell at 1.1 V vs RHE and at short circuit condition respectively.

Figure 1(a) shows the schematic diagram of the tandem device, in which perovskite solar cell is connected to the hematite photoanode externally. We employed a mesoporous perovskite solar cell (Figure S1) fabricated through double step procedure (J_{SC}= 17.72mAcm^{-2}, V_{OC}=1.11V; FF=0.53; PCE=10.5%) for the construction of the tandem device. We examine pristine and Mn doped nanostructured hematite photoanodes (Figure S2) of optimised thicknesses (pristine hematite ~ 350 nm and Mn doped hematite ~ 300 nm) (Figure S3) and two tandem configurations (TS1 and TS2) wherein they are combined with the perovskite solar cell. Co-Pi oxygen evolution catalyst was deposited on the Fe_2O_3 photoanodes to improve onset performance. The operating current density (J_{op}) of the tandem devices perovskite/pristine hematite (TS1) and perovskite/Mn doped hematite (TS2) were determined by the crossing point of the photocurrent densities of hematite photoanodes and perovskite solar cell with an active area of 0.12 cm^2.[31] For accuracy in estimating the operating current density, the J-V curves of perovskite solar cell were measured by placing the hematite photoanode before the solar cell to account for optical absorption by the hematite photoanodes as shown in Figure 1(a).

The operating current densities of the separate components and together in tandem have been calculated by the crossing point of two photocurrent densities curves. The value of the predicted operating current density in separate component measurements are 1.33 mAcm^{-2} and 2.33 mA cm^{-2} for perovskite/pristine hematite and perovskite/Mn doped hematite respectively (Figure S4), while in tandem configuration the operating current densities are 1.21 mAcm^{-2} and 1.93 mAcm^{-2} for perovskite/pristine hematite (TS1) and perovskite/Mn doped hematite (TS2) respectively (Figure 1(b)). The small inconsistency between these two measurements can be ascribed to the

losses inside the PEC chamber and electrolyte. The fill factor of the perovskite solar cell in the tandem configuration increases from 0.55 to 0.62 and 0.68 for TS1 and TS2 devices respectively. The performance of the tandem devices and hematite photoanodes were tested in 1M NaOH electrolyte without applying any additional bias in the two electrode configuration (Figure 1(c)) using chopped illumination (AM 1.5G 100mWcm^{-2}). The current density closely matches J_{op} extracted from Figure 1(b).

The solar to hydrogen conversion efficiency has been calculated using the equation;[32]

$$\eta_{STH} = \left(\frac{J_{op} \times 1.23 \times \eta_F}{P_{Solar}}\right) \qquad (1)$$

where J_{op} is the operating current density (mA/cm^2), η_F is the Faradaic efficiency (preliminarily assumed to be 100%) and P_{Solar} is the irradiance intensity of 100 mWcm^{-2} (AM1.5G). The STH efficiencies were calculated to be 1.5% and 2.4% for pristine hematite/perovskite solar cell (TS1) and Mn doped hematite/perovskite solar cell (TS2) respectively.

To understand the opto-electrical limitation in tandem devices, optical transmittance of hematite photoanodes has been measured to determine the remaining spectral response for perovskite solar cell. The transmittance and spectral response of hematite photoanodes were suitably matched with the reported hematite energy band gap (~ 2 eV). Incident photon to current conversion efficiency (IPCE) of each component in tandem device plays an important role in understanding the opto-electrical losses as well as the device performance. IPCE of hematite photoanodes were measured at 1.23 V vs RHE and at short circuit condition for perovskite solar cell (Figure 1(d)). IPCE can be expressed using the following equation:[20]

$$IPCE\ (\%) = \left(\frac{1240 \times I_{Ph}}{\lambda \times J_{Light}}\right) \times 100 \qquad (2)$$

Where I_{Ph} is the measured photocurrent density at a particular wavelength, λ is the wavelength of incident light, and J_{Light} is the measured irradiance at a specific wavelength. The solar spectrum incident on the perovskite solar cell can be calculated by multiplying the standard solar photon flux with the measured transmittance of hematite photoanodes (**Figure 2**).

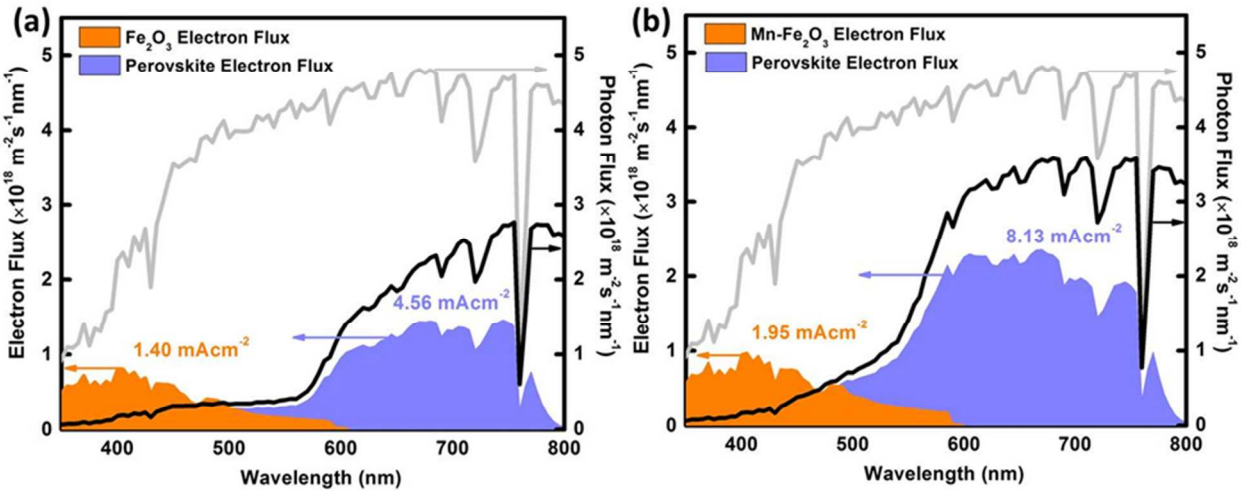

Figure 2.(a) Standard solar AM 1.5 G photon flux and incident photon flux for solar cell calculated by multiplying the standard photon flux by the transmittance of the hematite. The shaded areas are electron flux from pristine hematite and Perovskite solar cell used to calculate the integrated photocurrent density of hematite photoanodes. (b) Standard solar AM 1.5 G photon flux and incident photon flux for solar cell calculated by multiplying the standard photon flux by the transmittance of the Mn doped hematite. The shaded areas are electron flux from Mn doped hematite and Perovskite solar cell used to calculate the integrated photocurrent density of hematite photoanodes.

Electron flux of each light absorbing component can be calculated by multiplying the incident spectral response with its measured IPCE value. The electron flux calculation for hematite

photoanode is straight forward in comparison to the perovskite solar cell considering that the standard AM1.5G solar flux (100 $mWcm^{-2}$) is incident upon the photoanode. The calculated integrated current density of the individual pristine hematite/Perovskite and Mn doped hematite/Perovskite device combinations are 1.40 $mAcm^{-2}$ / 4.56 $mAcm^{-2}$ and 1.95 $mAcm^{-2}$ / 8.13 $mAcm^{-2}$ respectively. This therefore shows that although there is an overlap in the optical absorption for the two components in the tandem cell, the optical absorption within the Fe_2O_3 photoanode does not constrain the photocurrent generated by the perovskite solar cell. Moreover, the lower optimized thickness of the doped hematite further reduces the constraints on the photocurrent generated by the perovskite solar cell.

In order to estimate the Faradaic efficiency and the stability of the tandem device, we have performed gas evolution experiment in a twin (H_2 and O_2) PEC reactor under 1 Sun AM 1.5 G (100 mW cm^{-2}) irradiation in the tandem configuration. These experiments confirm that the photocurrent generated is translated to O_2 and H_2 at respective electrodes. We have measured the evolved gases from the tandem configuration continuously up to 8 hrs. The amount of evolved H_2 and O_2 with time is presented in **Figure 3** while the inset shows the photocurrent acquired during the gas evolution measurement. The theoretical amounts of evolved gases has been calculated by integrating the photocurrent with time while considering that the O_2 and H_2 evolution reactions are four-electron and two-electron processes respectively (straight lines in Figure 3). Based on the amount of O_2 evolved with time the calculated Faradaic efficiency was 95 % for our tandem device, matching previous reports. The 5% mismatch in Faradaic efficiency might be due to the manual sampling error.[11] Long term measurements of upto 8 hours were done, however due to the ambient humidity conditions (RH of 60-70%) the unencapsulated

perovskite solar cells decayed in performance and the photocurrent of the tandem cell dropped by 25%.

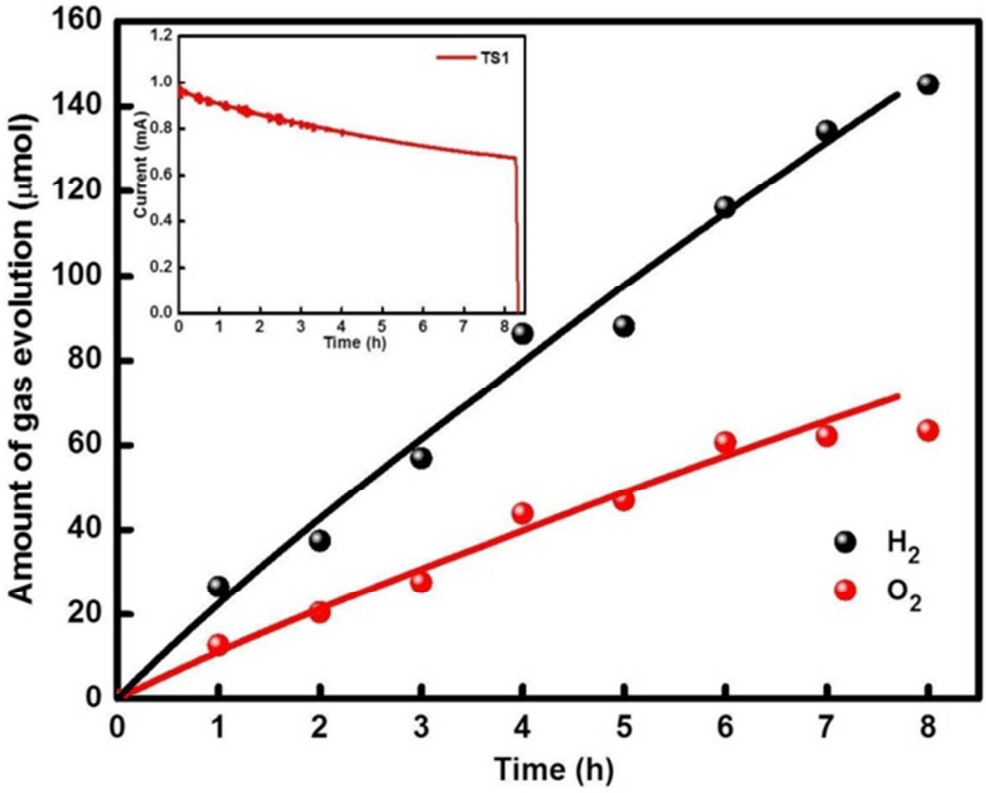

Figure 3. Faradaic efficiency measurement for tandem device TS1. Red and black symbols correspond to the O_2 and H_2 gases measured by gas chromatography while the black and red lines correspond to the integration of the photocurrent with respect to time. Inset shows the photocurrent measured during the gas evolution.

Our results clearly indicate that the perovskite solar cell- Fe_2O_3 tandem devices are able to perform light induced water splitting in the absence of an external applied bias. As indicated previously, the perovskite solar cell provides about 1.1 V of photopotential. However, an unassisted system requires a total voltage of about ~1.8V for efficient water splitting, with the

remaining photovoltage arising from the hematite photoanode. However, the Fe_2O_3 photoanode's contribution is not directly apparent from the STH efficiency calculations. The STH conversion efficiency quantifies the entire tandem cell and accounts for all the losses inside tandem cell and can be derived only for two electrode systems. This is because one cannot accurately define the potential drop between working and counter electrode. To evaluate the performance of our hematite photoanodes, the intrinsic solar to chemical conversion efficiency (ISTC) has been calculated based on our previous report.[32] This involves the characterisation of the Fe_2O_3 water splitting photoanodes separately by current-potential measurement using a three-electrode configuration with 1M NaOH electrolyte solution (pH 13.6) under dark and illumination. The photocurrent is calculated by the difference between light and dark currents i.e., $J_{photo} = J_L - J_D$ and the photovoltage is simply the potential difference between the light current and the dark current, as shown by the arrows in **Figure 4**(a). The photocurrent density at 1.23 V vs. RHE is 1.7 $mA.cm^{-2}$ for the pristine hematite photoanode and 3.5 $mA.cm^{-2}$ for Mn doped hematite. To obtain the intrinsic power to chemical conversion efficiency of pristine hematite and Mn doped hematite photoanodes, the intrinsic photovoltaic power of the hematite photoanodes were derived by the product of their photocurrent and photovoltage and multiplied by the chemical conversion rate (Supplementary Information). The intrinsic photovoltaic power density reaches a maximum of 0.82 $mWcm^{-2}$ at a potential of 1.22 V vs. RHE for pristine hematite and 3.0 $mWcm^{-2}$ at a potential of 1.3 V vs. RHE for Mn doped hematite (Figure S5 and S6). This corresponds to the electrical power conversion efficiency. However, the photoanode performs chemical work by splitting water in order to produce oxygen and electrons at the back contact for hydrogen production. Thus the total power to chemical conversion efficiency or intrinsic solar to chemical

conversion efficiency (ISTC) of hematite photoanode can be calculated by using the following equation;

$$ISTC = \frac{1.23(\mathrm{V_{RHE}})}{V_{dark}(\mathrm{V_{RHE}})}\left[\frac{J_{photo}(mAcm^{-2})\times V_{photo}(\mathrm{V})}{100(mWcm^{-2})}\right]_{AM1.5G} \quad (3)$$

where J_{photo} and V_{photo} are the photocurrent and photovoltage, while V_{dark} is the potential that need to be applied on the photoanode to reach the respective current. We have extracted the Faradaic efficiency of hematite photoanode from gas evolution experiment, which is nearly 100% for both pristine hematite and Mn doped hematite photoanodes. The efficiency of the individual photoanode reaches a maximum of 0.52% at a photocurrent density of 1.62 $mAcm^{-2}$ (at 1.22 V vs. RHE) for pristine hematite and 1.80% at a photocurrent density of 3.82 $mAcm^{-2}$ (at 1.3 V vs. RHE) for Mn doped hematite photoanode (Figure 4(b) and S7)). Since the onset potential of the Fe_2O_3 photoanodes are not favourable, the operating point of our tandem system does not coincide with the ISTC maxima.

By examining the data from linear scanning voltammetry curves (Figure 4(a)), it is possible to extract the photopotential generated by the water splitting anodes. In the dark the Fe_2O_3 anodes would have to be biased to a higher potential of 1.92 V vs. RHE and 2.07 V vs RHE to produce the same photocurrent as at 1.22 V vs RHE for pristine hematite photoanode and 1.29 V vs RHE for Mn doped hematite photoanode. This clearly indicates that illumination generates a photovoltage of 0.7 V (1.92-1.22V) in the pristine hematite photoanode and 0.77 V (2.07-1.3V) in the Mn doped hematite photoanode. These photovoltages in series with the photopotential provided by the perovskite solar cell (1.1V) leads to efficient unassisted water splitting. We have shown the role of Mn doping with hematite photoanode in our previous manuscript.[30]

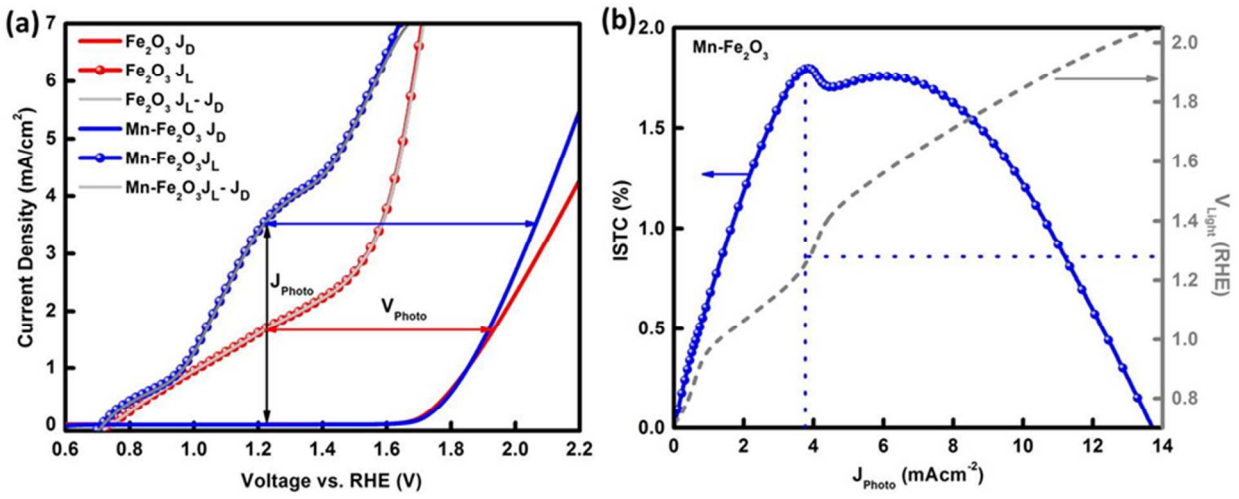

Figure 4. (a) Photocurrent – voltage curve of hematite photoanodes (pristine and Mn doped) in 1M NaOH electrolyte (pH 13.6) under 1 sun irradiation AM 1.5G (100 $mWcm^{-2}$) and (b) Intrinsic power to chemical conversion efficiency of Mn doped hematite photoanode.

CONCLUSION

We have demonstrated an efficient, stable, cost effective and simple water splitting D4 tandem PEC-PV cell with a STH efficiency of nearly 2.4% by combining the Mn doped Fe_2O_3 photoanode (Eg = 2.05 eV) and a single perovskite solar cell (Eg = 1.55 eV) in series. Systematic electro optical studies were performed to investigate the performance of tandem device. The photovoltage, internal photovoltaic power characteristics and the intrinsic solar to chemical conversion efficiency of hematite photoanodes have been extracted by linear scanning voltammetry curves under dark and illumination. The high open circuit voltages (1.1 V) generated by the perovskite solar cell in series with an efficient hematite photoanode resulted in unassisted light induced water splitting. Currently, the performance of the tandem system is limited by the low photocurrents generated by the water splitting photoanode. The primary limiting point of the system is the limited photocurrent production by the thin Fe_2O_3 photoanode.

Due to this, the operating point of the system is far away from the maximum power point of the solar cell. This limitation can be rectified by choosing smaller bandgap photoelectrodes[33] with efficient charge injection dynamics which would give higher photocurrents at low onset potential, or by designing light trapping structures[34, 35] which would improve optical absorption within the photoanode, while still allowing sufficient light absorption in the perovskite solar cell. The bandgap tunability of the halide perovskite family allows the design of a tandem device where a large bandgap perovskite solar cell could be utilised to drive smaller bandgap photoelectrodes. With the development of sufficient electrode stabilisation strategies, tandem systems which employ perovskite materials with Si photoelectrodes could yield STH efficiencies > 20%.

ASSOCIATED CONTENT

Supporting Information: Further measurement of analysis, ISTC calculation, FESEM surface morphology of hematite photoanodes and perovskite solar cell and sample images are available free of charge via the Internet at http://pubs.acs.org.

AUTHOR INFORMATION

Corresponding Author: Nripan@ntu.edu.sg

Present Addresses: School of Materials Science and Engineering, Nanyang Technological University, Nanyang Avenue, Singapore 639798.

Funding Sources

Financial support from the Centre of Artificial Photosynthesis via the Solar Fuels Lab at NTU and Singapore National Research Foundation (NRF) through the Singapore-Berkeley Research Initiative for Sustainable Energy (SinBeRISE) CREATE Programme is acknowledged. N.M. acknowledges support from NTU start-up grant M4081293 and the NTU-A*STAR Silicon Technologies Centre of Excellence under the program grant No. 112 3510 0003.

ACKNOWLEDGMENT

We would like to acknowledge Prof. Subodh Mhaisalkar for valuable discussions.

REFERENCES

(1) Crabtree, G. W.; Dresselhaus, M. S.; Buchanan, M. V. *Physics Today* **2004,** 57, 39-44.

(2) Fujishima, A.; Honda, K. *Nature* **1972,** 238, 37-38.

(3) Ohashi, K.; McCann, J.; Bockris, J. O. M. *Nature* **1977,** 266, 610-611.

(4) Weber, M. F.; Dignam, M. J. *J. Electrochem. Soc.* **1984,** 131, 1258-1265.

(5) Walter, M. G.; Warren, E. L.; McKone, J. R.; Boettcher, S. W.; Mi, Q.; Santori, E. A.; Lewis, N. S. *Chem. Rev.* **2010,** 110, 6446-6473.

(6) Butler, M. A.; Ginley, D. S. *J. Mater. Sci.* **1980,** 15, 1-19.

(7) Zeng, K.; Zhang, D. *Prog. Energy Combust. Sci.* **2010,** 36, 307-326.

(8) Bard, A. J.; Fox, M. A. *Acc. Chem. Res.* **1995,** 28, 141-145.

(9) Tachibana, Y.; Vayssieres, L.; Durrant, J. R. *Nature Photon.* **2012,** 6, 511-518.

(10) Khaselev, O.; Turner, J. A. *Science* **1998,** 280, 425-427.

(11) Brillet, J.; Yum, J.-H.; Cornuz, M.; Hisatomi, T.; Solarska, R.; Augustynski, J.; Graetzel, M.; Sivula, K. *Nat Photon* **2012,** 6, 824-828.

(12) Jacobsson, T. J.; Fjallstrom, V.; Sahlberg, M.; Edoff, M.; Edvinsson, T. *Energy Environ. Sci* **2013,** 6, 3676-3683.

(13) Rocheleau, R. E.; Miller, E. L.; Misra, A. *Energy Fuels* **1998,** 12, 3-10.

(14) Reece, S. Y.; Hamel, J. A.; Sung, K.; Jarvi, T. D.; Esswein, A. J.; Pijpers, J. J. H.; Nocera, D. G. *Science* **2011,** 334, 645-648.

(15) Abdi, F. F.; Han, L.; Smets, A. H. M.; Zeman, M.; Dam, B.; van de Krol, R. *Nat Commun* **2013,** 4.

(16) Bassi, P. S.; Gurudayal; Wong, L. H.; Barber, J. *PCCP* **2014,** 16, 11834-11842.

(17) Warren, S. C.; Voïtchovsky, K.; Dotan, H.; Leroy, C. M.; Cornuz, M.; Stellacci, F.; Hébert, C.; Rothschild, A.; Grätzel, M. *Nat Mater* **2013,** 12, 842-849.

(18) Hisatomi, T.; Dotan, H.; Stefik, M.; Sivula, K.; Rothschild, A.; Grätzel, M.; Mathews, N. *Adv. Mater.* **2012,** 24, 2699-2702.

(19) Sivula, K.; Le Formal, F.; Grätzel, M. *ChemSusChem* **2011,** 4, 432-449.

(20) Murphy, A. B.; Barnes, P. R. F.; Randeniya, L. K.; Plumb, I. C.; Grey, I. E.; Horne, M. D.; Glasscock, J. A. *Int. J. Hydrogen Energy* **2006,** 31, 1999-2017.

(21) Kumar, M. H.; Mathews, N.; Boix, P. P.; Nonomura, K.; Powar, S.; Ming, L. Y.; Graetzel, M.; Mhaisalkar, S. G. *Energy Environ. Sci* **2013,** 6, 3280-3285.

(22) Dotan, H.; Sivula, K.; Gratzel, M.; Rothschild, A.; Warren, S. C. *Energy Environ. Sci* **2011,** 4, 958-964.

(23) Klahr, B.; Gimenez, S.; Fabregat-Santiago, F.; Bisquert, J.; Hamann, T. W. *J. Am. Chem. Soc.* **2012,** 134, 16693-16700.

(24) Lin, Y.; Yuan, G.; Sheehan, S.; Zhou, S.; Wang, D. *Energy Environ. Sci.* **2011,** 4, 4862-4869.

(25) Jeon, N. J.; Noh, J. H.; Kim, Y. C.; Yang, W. S.; Ryu, S.; Seok, S. I. *Nat Mater* **2014,** 13, 897-903.

(26) Laboratory, N. R. C. E. R. b. N. R. E. NREL Research Cell Effeciency Records by National Renewable Energy Laboratory. http://www.nrel.gov/ncpv/images/efficiency_chart.jpg

(27) Xing, G.; Mathews, N.; Sun, S.; Lim, S. S.; Lam, Y. M.; Grätzel, M.; Mhaisalkar, S.; Sum, T. C. *Science* **2013,** 342, 344-347.

(28) Xing, G.; Mathews, N.; Lim, S. S.; Yantara, N.; Liu, X.; Sabba, D.; Grätzel, M.; Mhaisalkar, S.; Sum, T. C. *Nat Mater* **2014,** 13, 476-480.

(29) Luo, J.; Im, J.-H.; Mayer, M. T.; Schreier, M.; Nazeeruddin, M. K.; Park, N.-G.; Tilley, S. D.; Fan, H. J.; Grätzel, M. *Science* **2014,** 345, 1593-1596.

(30) Gurudayal; Chiam, S. Y.; Kumar, M. H.; Bassi, P. S.; Seng, H. L.; Barber, J.; Wong, L. H. *ACS Appl. Mater. Interfaces* **2014,** 6, 5852-5859.

(31) Chen, Z.; Jaramillo, T. F.; Deutsch, T. G.; Kleiman-Shwarsctein, A.; Forman, A. J.; Gaillard, N.; Garland, R.; Takanabe, K.; Heske, C.; Sunkara, M.; McFarland, E. W.; Domen, K.; Miller, E. L.; Turner, J. A.; Dinh, H. N. *J. Mater. Res.* **2010,** 25, 3-16.

(32) Dotan, H.; Mathews, N.; Hisatomi, T.; Grätzel, M.; Rothschild, A. *J. Phys. Chem. Lett.* **2014,** 5, 3330-3334.

(33) Li, Z.; Luo, W.; Zhang, M.; Feng, J.; Zou, Z. *Energy Environ. Sci* **2013,** 6, 347-370.

(34) Dotan, H.; Kfir, O.; Sharlin, E.; Blank, O.; Gross, M.; Dumchin, I.; Ankonina, G.; Rothschild, A. *Nat Mater* **2013,** 12, 158-164.

(35) Warren, S. C.; Thimsen, E. *Energy Environ. Sci* **2012,** 5, 5133-5146.

For TOC only